Sub-grid scale orography parametrizations

Philippe Bougeault

CNRM, Météo-France

Toulouse France

1. Introduction

The representation of unresolved orographic effects is one of the most difficult problems in meteorological models because of the large variety of processes involved. Orography modifies the mean flow by creating obstacles and additional turbulence, generates all kinds of waves, constitutes an elevated source of heat and moisture, traps low-level clouds within valleys, impacts on the distribution of rainfall, and even influences the radiative budget by slope and sky-masking effects. Most of these processes are purely ignored in larger-scale models of the atmosphere, and in this short contribution, I will concentrate on first-order dynamic effects. Some currenty used parameterizations are summarized in sections 2 to 5, followed by a discussion of key issues for the future in section 6. The last section presents briefly the Mesoscale Alpine Programme, and how it could help in this matter.

In recent years, the representation of dynamic effects of sub-grid scale orography (SSO) has been attempted by a variety of means, ranging from enhanced terrain, effective roughness, gravity-wave drag and lift, and occasionally enhanced turbulence production and characteristic length scales. Reviews of the subject can be found in Baines (1995), Beau (1997), and an ECMWF Workshop on Orography (1997).

A good introduction to the discussion of flow deceleration by orography is provided by the classical decomposition in Figure 1 (from Emeis, 1990). Here we consider only horizontal forces, assuming that the vertical component is balanced by the weight of the atmosphere. From basic fluid mechanics, we know that the force exerted by the flow on any obstacle (equal and opposite to the force exerted by the obstacle on the flow, by Newton's third law) consists in a viscous drag and a pressure drag. On a perfectly flat terrain the viscous drag is the only contribution, but in the case of the atmosphere, it is extremely small because the viscosity of the air is small. In fact, the largest part of the surface friction existing on flat terrain comes from the turbulence generated by small surface obstacles, and even if we represent it by a "roughness height" it is basically a pressure drag effect. The pressure drag is often divided in two components: the drag (parallel to the flow) and the lift (perpendicular to the flow). The Coriolis force is one main reason for lift effects, but even in the absence of rotation, large lift effects are usually present because of obstacle asymmetry. Alternatively, the drag is often considered as a vector, with zonal and meridian components, thereby including the lift effects. We will return on this decomposition problem in Section 6. The drag is next split in three parts. First, the "hydrostatic drag" is that part that would exist in absence of any motion. It is purely generated by the hydrostatic pressure difference between the two sides of an obstacle, as observed for instance when large temperature differences exists between the northern and southern sides of a range.

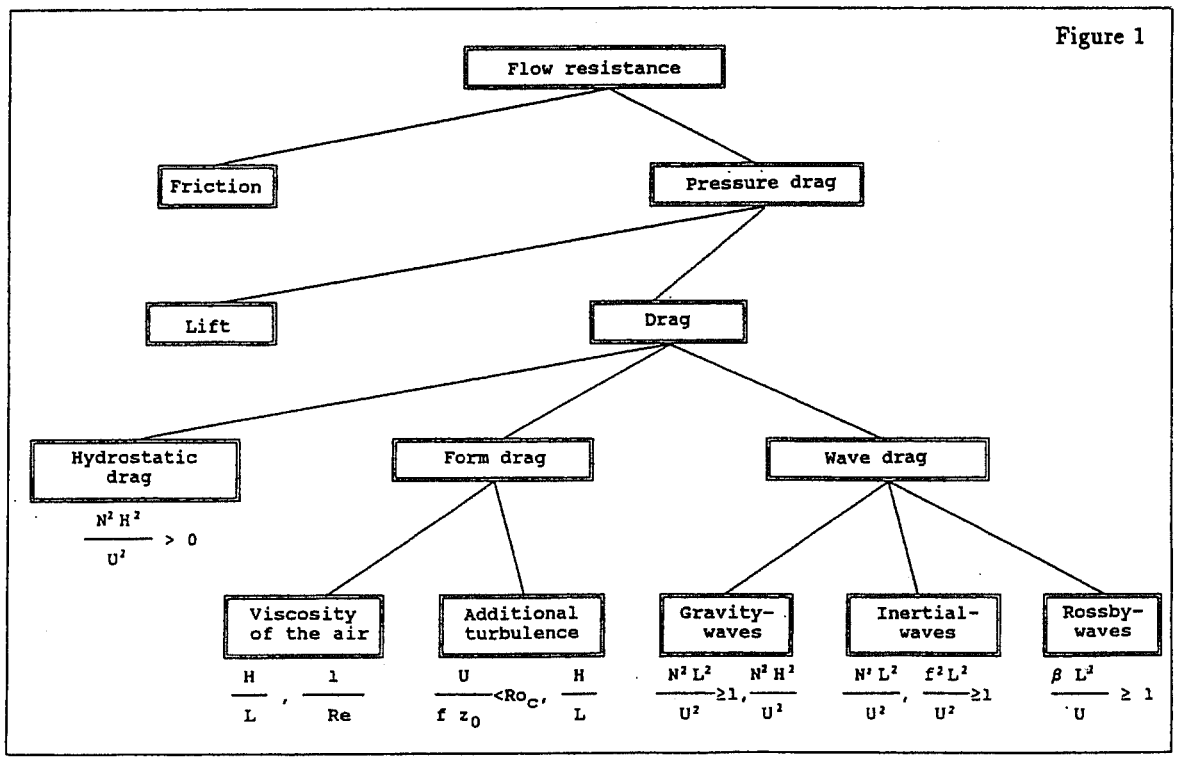

Figure 1: Different contributions to the flow resistance (after Emeis, 1990).

The hydrostatic drag is generally considered to be related to the larger scales of the flow, and should therefore be relatively well represented by the resolved flow. I do not know of any attempt to parameterize this effect, however there does not seem to be any definite proof that this is sufficient. The "form drag" is the part of the drag that is directly related to the pressure difference on the upstream and downstream sides of the obstacles, in presence of a well-defined mean flow. The evaluation of form drag effects is a central problem in classical fluid mechanics, and numerous theoretical models are available. The form drag is associated to a local deceleration of the mean flow. Finally, the wave drag is the part of the drag which is due to the generation of waves by the obstacles, and we know of at least three types of such waves: gravity waves, inertial waves and Rossby waves. The wave drag is associated to a deceleration of the mean flow which is not necessarily local, and can occur at some distance from the mountain (vertical or horizontal) because the waves can transport momentum. As we will discuss in Sections 3 and 4, it turns out that the current practice is to have no separate representation of the form drag in atmospheric models. The form drag generated by smaller obstacles is included in an "effective roughness" concept and treated together with the viscous and turbulent friction. The form drag generated by larger obstacles is somehow included in the gravity-wave schemes (blocked flow effects). Finally, it is often admitted that Rossby waves and inertial waves are explicitly represented in atmospheric models, so that only the smaller-scale gravity-waves need to be parameterized.

2. Enhanced orography

At the beginning of the 80s, several systematic errors in the representation of the mean zonal flow and the planetary waves were noted in GCMs and attributed to an insufficient representation of orography. Early solutions to these problems relied on enhanced orography techniques. Indeed, linear theory shows that the response of the flow to the orography often depends primarily on the maximum height of a range. Let h be this maximum height, the non-dimensional parameter governing the linearity of the flow is Nh/U, where N

and U are the low-level buoyancy frequency and wind speed. When the topography is averaged to the resolution of the dynamic model, the total volume is conserved rather than the maximum height, which may degrade the representation of linear waves. Another argument was the observation that the flow in deep valleys is often decoupled from the flow at higher altitude, suggesting that the effective volume of the mountain, as seen by the larger scale flow, should include the volume of the deepest valleys. This has been exploited in several sudies. One of the first attempts was the valley-filling technique of Mesinger (1977). In the envelope orography technique of Wallace et al (1983), the effective height of the mountain at each grid point of the model is assumed to be the mean height plus the standard deviation within the grid (multiplied by some empirical coefficient of order one). This very simple parameterization was quite successful and came to be used in many models during several years, because it greatly improved the stationary planetary wave pattern. An alternative technique proposed by Mesinger and Collins (1986) relies on the computation of the silhouette of the orography as seen by the flow, depending on its direction. This later technique is quite appealing because it relies on objective computations, and does not suffer from some drawbacks of the envelope orography: for instance the boundaries of large mountain ranges correspond to the largest standard deviations, which may generate unphysical maxima of envelope orography, a problem which does not exist in the silhouette technique.

However, the use of these techniques has declined with the development of more detailed representations of the pressure drag. In addition, the use of high mountains in models is detrimental for the data assimilation process: indeed, in mountainous areas, most observations are performed in the valleys, and their use is made more difficult if the forecast model has an artificially high orography.

3. Effective roughness height

A rather obvious method to account for the existence of the SSO is to consider each detail of the topography as an additional roughness element, and to define a large "effective roughness height". In the theory of the turbulent boundary layer, the roughness height z_0 is defined only in reference to the logarithmic wind profile

$$u(z) = (u_* /k) \, \mathrm{Ln} \, (z/z_0) \, , \qquad (1)$$

where u_* is the friction velocity and k the Karman constant. So, the proper definition of effective roughness heights ultimately relies on the actual existence of such profiles above mountains. Fortunately, there is some experimental evidence of log profiles above small hills (e.g. Kustas and Brutsaert, 1986; Grant and Mason, 1990). In this case, we expect the effective roughness height z_0^{eff} to depend on the background roughness z_0, on the mean height of the obstacles, represented by the standard deviation of the SSO, σ_h , and on the shape and density of the obstacles. This may introduce a large number of parameters, such as characteristic horizontal length scales, slopes, aspect ratios, etc... There are numerous studies of the resistance to the flow exerted by various obstacles, and these show that the flow regime, hence the effective roughness definition, depend on the maximum value of the slopes. For small slopes, the effective roughness remains proportional to the background roughness, with an enhancement factor depending on the slope. For large slopes, the resistance to the flow is governed by the frontal area of the obstacles and some drag coefficients.

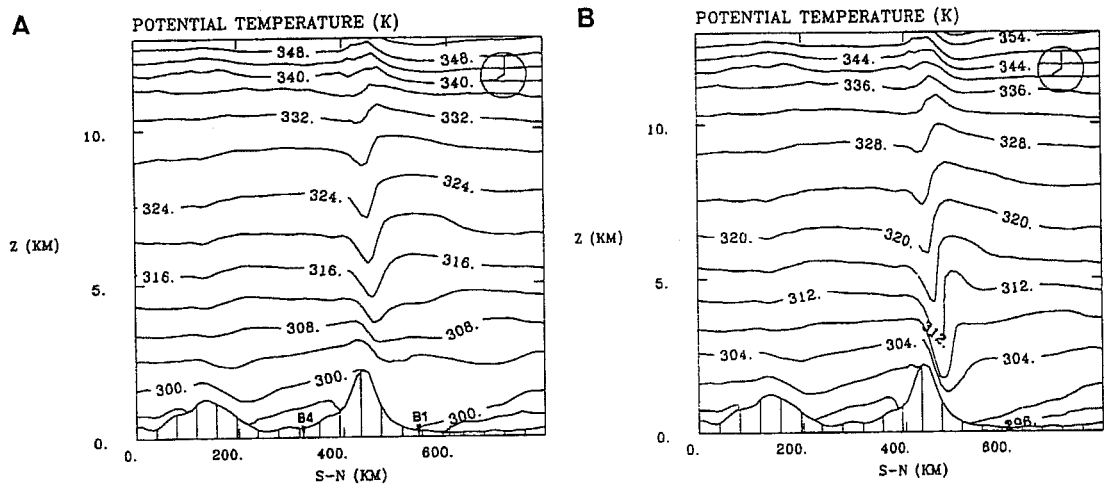

Figure 2: Cross-section of the isentropes for a mountain wave above the Pyrénées, with (A) and without (B) effective roughness (after Georgelin et al., 1994)

The method proposed by Mason (1986) was used by Georgelin et al. (1994) in a numerical study of a deep mountain wave observed during the PYREX experiment (Bougeault et al., 1997). Figure 2, from this study shows the impact of the effective roughness height. Although this was obtained with a 10km grid size model, it is believed that results are valid for larger grid size models as well. On the right panel, the usual roughness height is used (about 0.5 m) and the amplitude of the mountain wave is largely overestimated as compared to the available observations (not shown). On the left panel, the effective roughness height is used, resulting in $z_0^{eff} \approx 15$ m, and the mountain wave has about the right magnitude. Moreover, the effects of effective roughness height in mountainous areas have been further evaluated during an international inter-comparison of limited-area models, held within the COMPARE program framework. In this program, a number of LAMs have simulated a case from PYREX, with identical domain, resolution, initial and boundary conditions. In one of the experiments, the definition of the orography and of the roughness was left to the initiative of the participants. Results published by Georgelin et al. (2000) clearly establish the benefit of large roughness heights over the meso-scale Pyrenean mountain range. Indeed all of the best-ranking models used the effective roughness height concept, while most of the worst-ranking models alternatively used the envelope orography concept.

Recent work on the effective roughness height concept has been based on large eddy simulation models. As an example, Wood and Mason (1993) propose a rather complex formula, which fits well a number of highly resolved simulations performed with a 3D model on various mountain shapes (2D ridges, 3D periodic mountains, 3D isolated mountains, with both small or large slopes). This reads approximately:

$$\mathrm{Ln}\,(z_m/z_0^{eff}) = \mathrm{Ln}\,(z_m/z_0) \,/\, \left(1+\alpha\,\beta\,\pi^2\,(A/S_h)\,(A/S_d) \right)^{1/2} \qquad (2)$$

Here, z_m is the maximum of the mountain height and of h_m (a complex function of λ/z_0, of order 100 m), λ is the characteristic horizontal length scale of the topography, and A is the frontal area of the topography. Note that the use of A introduces a clear directional dependence in the definition of z_0^{eff} . S_h is the surface of the orography elements, S_d is the area of the grid box. α is a O(10) coefficient depending on (λ/z_0^{eff}), and β is a O(1) coefficient depending on the mountain shape. Because of its complex formulation, Eq. (2) is currently only used in the UKMO model under a simplified form, for instance the directional effects are averaged out. This formulation results in values of several tens of meters over the Alps.

4. Gravity wave drag

The existence of a pressure drag on obstacles due to the emission of waves has been known for a long time (e.g. Queney, 1948), but the importance of the flow deceleration in altitude due to wave breaking was only realized in the last twenty years. A good general presentation of the problem of gravity-wave drag parameterization and early solutions can be found in Palmer et al. (1986). The two basic problems are to evaluate the surface pressure drag τ and to compute the vertical distribution of the wave momentum flux, that will generate the mean flow deceleration. The linear theory of stationary mountain waves has been extensively used as a guide to these expressions. An excellent pedagogical introduction to this theory may be found in Mobbs (1994) and I will not repeat it here.

In the case of uniform flow over a 2D, bell-shaped mountain, the linear, hydrostatic, pressure drag at the surface is given by

$$\tau = (1/L)\,(\pi/4)\,\rho\,U\,N\,h^2\,, \tag{3}$$

with ρ the flow density in low levels, N the buoyancy frequency, U the mean velocity, h and L the vertical and horizontal dimensions of the mountain. This turns out to be the maximum value over the whole regime of the non-dimensional parameter NL/U, and is obtained for NL/U≈5-10 (see e.g. Fig. 8.10 in Gill, 1982). In the standard atmosphere, this corresponds to L≈10km. The value of the drag is cut down by non-hydrostatic effects for smaller L and by rotation effects at larger L.

An early attempt to model the surface pressure drag generated by mountain waves was in Boer et al. (1984), proposing the (vectorial) formula

$$\tau = K\,\rho\,N\,U\,\sigma_h\,, \tag{4}$$

where σ_h is the SSO standard deviation. In this study, K is a non-dimensional numerical coefficient equals to $2\ 10^{-3}$. This formula did not follow the linear theory for mountain waves, which rather dictates an h^2 dependency for τ (Eq. 3). Further works rather used the more classical formula

$$\tau = K\,\rho\,N\,U\,\sigma_h^{\,2}\,, \tag{5}$$

where K is now a dimensional coefficient accounting for the mountain horizontal scale. In McFarlane (1987), $K= 8.\ 10^{-6} m^{-1}$, and in Palmer et al. (1986), $K=2.5\ 10^{-5}\ m^{-1}$. Bougeault et al (1993) showed from PYREX data that K should in fact take larger values (four times larger), a result that was confirmed later on by Lott and Miller (1997).

The micro-barograph data from PYREX have been used to explore the validity of these linear estimates. The drag across the Pyrénées was computed by Bessemoulin et al (1993). It varies from 8Pa (case of strong northerly flow) to –6Pa (case of strong southerly flow). In Figure 3, the observed drag is shown to agree extremely well with the result of Eq. (3). This comes as a surprise, since the theory is valid for a 2D, linear case ($Nh/U \ll 1$), while the Pyrenees are 3D and Nh/U is often larger than one in the considered cases. A possible explanation for this paradox was offered by Olafsson and Bougeault (1997), who showed that there is a compensation between friction and rotation effects, that keeps the drag close to the linear 2D results for a wide range of values of Nh/U (see Figure 4).

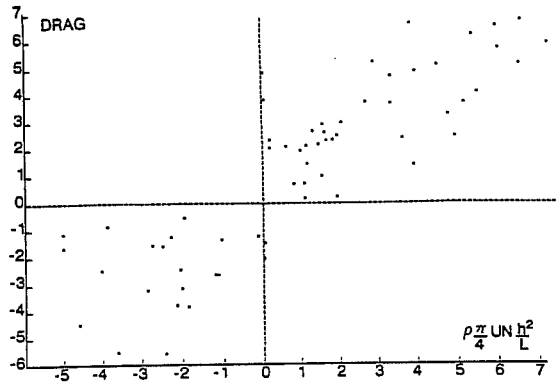

Figure 3: Surface pressure drag (Pa) measured (y axis) and estimated by the linear 2D formula (x axis). From Bessemoulin et al.(1993).

An additional complexity is due to the consideration of the directional effects over three dimensional topography. Phillips (1984) computed the drag components for a uniform U and N flow over elliptical isolated mountains. Based on this work, Baines and Palmer (1986) computed the two components of the surface drag vector as

$$\tau_{//} = k\,\rho\,N\,U\,\sigma_h^2\,(B(\gamma)\cos^2\psi + C(\gamma)\sin^2\psi)\,,$$
$$\tau_{\perp} = k\,\rho\,N\,U\,\sigma_h^2\,(B(\gamma) - C(\gamma)\sin\psi\cos\psi)\,, \qquad (6)$$

where γ measures the anisotropy of the SSO, ψ the angle between the low level flow U and the direction of the largest slope, and B and C are known functions. An alternative computation has been recently proposed by Gregory et al. (1998).

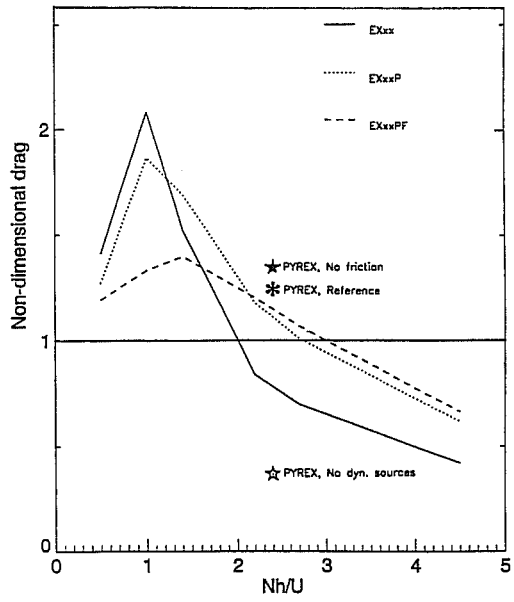

Figure 4: Surface pressure drag (normalized by the 2D, linear value) as function of the non-dimensional mountain height (Nh/U) for several numerical experiments. Full line: without rotation and friction; dotted line: with rotation but without friction, dashed line: with rotation and friction. The other symbols note the value recovered in realistic runs initialized with PYREX analyses, and come close to the idealized experiments. After Olafsson and Bougeault (1997).

The second problem for GWD parameterizations is to evaluate how the associated wave momentum flux varies with height, knowing that the mean flow will vary in proportion to the vertical derivative of the momentum flux. One basic result of the linear theory is the Eliassen-Palm theorem, which states that for a steady wave in the absence of dissipation, the wave momentum flux is constant with height as long as the mean wind projected in the direction of the wave vector is not zero (linear critical level). See e.g. Mobbs (1994) for a demonstration. At critical levels, on the contrary, waves amplify because the vertical group velocity becomes very small. The amplification leads to breaking and absorption by turbulence. Thus, waves are destroyed at critical levels and deposit their momentum flux at this height, generating mean flow deceleration. Waves can also amplify with height due to the mean density decrease, leading again to breaking and mean flow deceleration. The two effects are embodied in the saturation theory of Lindzen (1981), which forms the basis for most parameterizations of the vertical variation of the wave-momentum flux. Lindzen made the hypothesis that turbulent mixing maintains the isentropes exactly vertical within the breaking areas, and showed that under this condition, the momentum flux has a maximum value of

$$\tau_{sat}(z) = - (1/2)\, \rho\, k\, U^3 / N, \tag{7}$$

where k is the dominant horizontal wave number, and ρ, U and N are the density, wind and stability at altitude z. On the other hand, the momentum flux is related to the wave amplitude, measured by the local vertical deviation of the isentropes ζ, by the equation

$$\tau(z) = - (1/2)\, \rho\, k\, U\, N\, \zeta^2 . \tag{8}$$

The computation of the vertical variation of the momentum flux relies on (7), and goes sequentially from the surface to the top of the atmosphere. For each level, the flux is kept at the same value as the level immediately below, if this value is less than the local value of the saturation flux. If the saturation flux is exceeded, waves are assumed to break and adjust to the saturation flux value, and the flux takes this new value, etc.. The local amplitude of the waves is deduced from (8). Only the general principle is given here, in practice the computation is fairly complex, in order to account for the respective directions of the wind and wave number vectors .

Additional complexities exist in more recent schemes due to consideration of blocking, 3D critical levels, lee waves and resonances. In presence of weak low-level wind, strong stability, or high SSO, (3) does no longer provide an adequate lower boundary condition for the wave momentum flux, because the actual flow will go around the individual mountains rather than above. This occurs when the non-dimensional height of the mountains Nh/U is close to one or larger, and the height of the layer diverted around the mountain is given, according to a formula due to J. Hunt, by

$$Z_b \approx \max (0, h\,(1 - U/Nh)). \tag{9}$$

This could also be validated during the PYREX experiment (see Figure 5). In this case, the layers below Z_b are not subject to a gravity wave stress, but rather to a form drag deceleration effect. This has been exploited by Lott and Miller (1997) to design the present GWD scheme of the ECMWF model. In this scheme Z_b is defined through a generalization of (9) to account for the vertical variations of U and N in the low levels following

$$\int_{Zb}^{3\sigma} \frac{N}{U} dz \approx 1 . \tag{10}$$

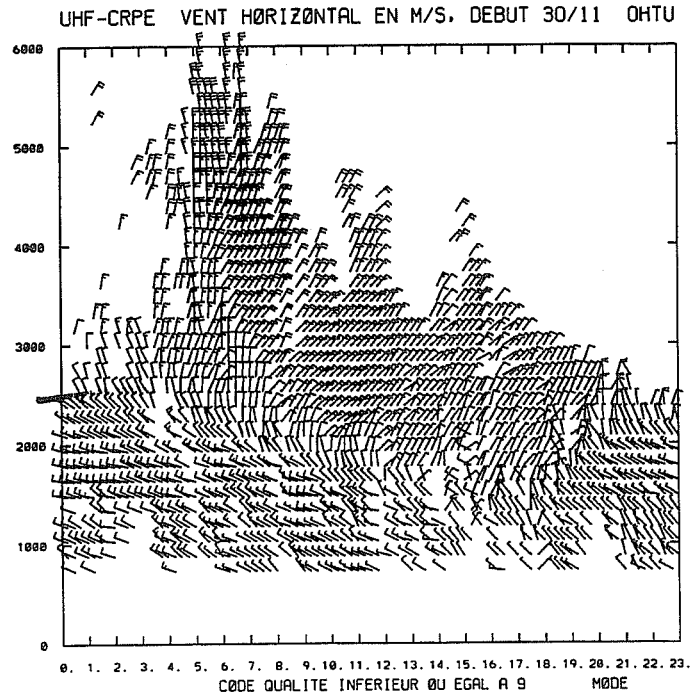

Figure 5: Wind velocity observed by a wind profiler upstream of the Pyrénées during PYREX. The shear line between the flow going above the mountain and the flow around is clearly visible, and the altitude was shown to coincide with Eq.(9) (M. Petitdidier, personal communication).

Below Z_b, the flow is subject to a drag varying as Z_b-z on the vertical, and depending on the mean anisotropy of the obstacles. Above Z_b, the above mentioned gravity-wave drag is applied.

The effects of change in the direction of the mean wind have been examined by Shutts and Gadian (1997). If the wind direction changes with height, the Eliassen-Palm theorem does not hold in general since wave vectors at right angles to the flow are subject to critical level absorption. This is particularly important above a complex, 3D topography, since the wave fields contains wave vectors in all directions. A simple prototype problem was examined with an isolated circular mountain and a wind field of constant speed with direction varying linearly in z. Figure 6 compares analytical linear solutions and numerical solutions for the wave momentum flux in this case, and shows that the flux vector is changing in direction and length at all altitudes. An adaptation of the UK meteorological office parameterization scheme was proposed to account for this effect. The significance of this is not yet established, as such strong directional shears are not very common in the earth atmosphere.

Lee waves occurs when the wave energy is trapped in a given altitude band by rapid variation of the mean profiles of U and N with height. In this case the mean flow can be significantly modified well downstream of the mountain range. These effects have been explored in high resolution simulations by Héreil and Stein (1997). Finally, resonances occur when a non-linear wave breaking level is separated from the surface by a certain number of wave lengths. In this case, a downslope windstorm develops, leading to a very strong pressure drag at the ground. The mean flow is then strongly decelerated in the altitude range extending from the ground to the breaking level (although the local flow is accelerated on the foothills). These two effects are accounted for in modern parameterization schemes, but the extent to which they influence the general circulation is not known.

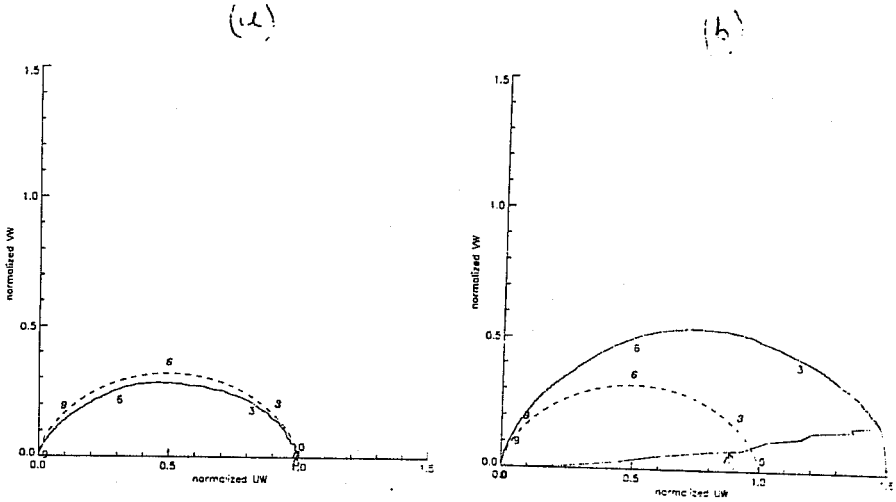

Figure 6: Polar plot of the normalized vertical momentum flux for (a) a 100 m hill and (b) a 1km hill. Analytical curves are given by the dashed lines, numerical results by the full line. The numbers indicate the height in km. After Shutts and Gadian (1997).

5. Possible lift effects

Mountains exert on the atmosphere a lift force L perpendicular to the mean flow, which is to first order proportional to the earth rotation and to the mountain volume V (Smith, 1979):

$$L = -\rho f U V. \tag{11}$$

Recently, Lott (1997) examined the response of planetary flow to a simple parameterization of lift forces based on the above formula. In his simulation, the mountains were removed from the model and replaced either by a low-level drag parameterization or by a low-level lift parameterization based on (11). He found that the lift was more effective at reconstructing the observed planetary wave pattern. This can be expected from simple quasi-geostrophic arguments, since the prime effects of mountains on balanced flows is to change the vorticity (maintaining the potential vorticity constant). At first sight these results are not much more than a curiosity and would imply that as long as the mountain volume is well represented in models, the lift forces will be accurate (this is pleading for the use of mean orography). However, one possible implication is that if the effective mountain volume seen by the large scale flow is larger than the true volume (by inclusion of parts of the valleys), the lift forces may be underestimated. This may explain why the early results with enhanced orography were so successful, and suggest that the use of mean orography (exact mountain volume) may have to be complemented by some parameterization of the unresolved lift effects. This is still a very prospective subject.

6. Summary of usage in various models

Table 1 Table 1: Summary of present usage of parameterizations in some NWP and climate models.summarizes the present definition of SSO parameterizations in several models. It can be seen that enhanced orographies are now the exception, while effective roughness heights and gravity wave drag parameterizations are common. Only the climate version of the Arpege model at Météo-France uses a lift parameterization. The JMA model uses a specific parameterization to increase the turbulence mixing length instead of the effective roughness length approach.

	Enhanced orogr	Eff. roughness	GWD	Lift
ECMWF	No	Yes Z0h=0.1*z0	Lott and Miller (1997)	No
UKMO	No	Wood and Mason (1993) Mason(1991) for scalars	Gregory et al (1998) with modifications	No
DWD	No	Yes, $f(\sigma_h)$, same for scalars except different limits	Lott and Miller (1997)	No
JMA	No	No, but σ_h used in the turbulence mixing length	Iwasaki et al (1989)	No
NCAR	No	No	McFarlane (1987)	No
Météo-France	Yes (mean+σh)	Geleyn and Tibaldi (0.53*slope*σh) Z0h=0.1*z0	Boer et al (1984) with modifications, Geleyn et al (1994)	In climate model only (Lott, 1999)

Table 1: Summary of present usage of parameterizations in some NWP and climate models.

7. Some important issues

The increasing use of complex formulations such as (2) or (6) introduces a strong dependence on higher-order aspects of the terrain distribution (slopes, characteristic scales, anisotropy, etc...). In many models, this statistical description of the SSO is somewhat different in the effective roughness approach, where frontal obstacle areas and characteristic horizontal length scales are favored (e.g. Eq. 2), and in the GWD approach which adopts a description based on slopes, anisotropy, and standard deviation (e.g. Eq. 6). This is an obvious source of confusion, and it would be beneficial to look for a unified description of the terrain properties.

Furthermore, these higher-order properties of the SSO depend heavily on the accuracy and resolution of the reference orographic dataset used to evaluate them. Taylor et al. (1997) noted a lack of convergence of the higher-order properties of the SSO over a given domain when the resolution of the reference orographic data-set is increased. There is an increased need for high-quality, high-resolution orographic datasets. This is an obvious problem to solve before any definitive work can be done on the parameterizations themselves.

The consideration of the blocked flow drag within the GWD parameterization is to some extent redundant with the form drag of obstacles described by the effective roughness length. In order to avoid double counting, it is recommended (e.g. ECMWF Workshop on Orography, 1997) to make a clear separation of horizontal scales in the SSO: the scales smaller than a few km should be accounted for in the effective roughness length, while the scales of 5 km and above, which can generate mountain waves, should be accounted for in the GWD. Still, the transformation of a volume force into a surface force which is accomplished through the effective roughness height concept remains somewhat artificial. One may argue that a unified approach of the form drag as a volume force is needed, and will eventually replace the effective roughness length and the blocked flow part of the GWD.

Validation is a major concern for SSO parameterizations. It is virtually impossible to acquire observations directly useful to test these formulations. For the effective roughness, the measurement of turbulent fluxes of momentum by aircraft would require long flight tracks (to achieve statistical convergence, necessary for an accurate estimate of the fluxes) far from the surface (well above the estimated values of z_0^{eff}). But the

underlying surface is rarely homogeneous on a sufficiently large area for these flights to be possible. For the GWD, direct observations of the wave momentum fluxes by aircraft are only possible along specific lines, while the quantities of interest are averages within horizontal planes. Over 3D topography, line and plane averages can be very different (e.g. Satomura, 1996). Additional problems come from the need to acquire such measurements at several altitudes simultaneously.

Diagnostics from highly resolved numerical simulations appear to be the main source of validation in the near future. Several studies have attempted this in the past. It appears necessary to make a careful distinction between the resolved and parameterized parts of the flow. To achieve a clear separation, Beau and Bougeault (1998) have developed a technique of differential momentum budgets which is recommended. They treated only four cases from PYREX, but this was sufficient to exhibit large errors in some parameterizations. For instance, the Arpege parameterization, based on Eq. (7), was not able to reproduce the wave momentum flux, while the (then operational) parameterization of the ECMWF, based on an empirical linear decrease of the flux, was giving better agreement after tuning. A full discussion of momentum budgets in presence of lee waves, over 2D and 3D orography, is provided by Héreil and Stein (1997, 1999). It is recommended to conduct more similar studies on realistic cases from field experiments, such as PYREX, because it is then possible to examine the realism of the simulations by direct comparisons with observations. For instance the model momentum fluxes obtained along the flight tracks can be validated through direct comparison with aircraft observations, then the momentum fluxes in horizontal planes are used to validate GWD parameterizations.

Several aspects of SSO parameterizations could be improved by taking advantage of the outstanding dataset acquired during the Mesoscale Alpine Programme. Contrarily to PYREX, the MAP was not directly aiming at improving the SSO parameterizations in large-scale models. However, a large number of high-resolution experiments will be achieved by various groups in the frame of MAP, and they could be used to validate parameterizations. An overview of MAP is provided in the next section.

Other current problems in the definition of effective roughness lengths can be summarized as follow:

- The introduction of directional roughness height has to be done in models in a careful way, and implications have to be studied.
- The dependence on stability needs to be assessed, and this is difficult in the frame of the Monin-Obukhov theory, because this one assumes that the roughness height is much smaller than the Monin-Obukhov length, which is no longer true for large roughness heights.
- Roughness heights for heat and moisture must remain much smaller than the dynamic ones, and there is a lack of theoretical guidance to compute adequate values.

A similar list for GWD parameterizations:

- It is not clear at which level U and N should be estimated to evaluate the surface pressure drag. The interaction of the wave field with the presence of the PBL (and possibly of clouds) should be explicitly represented. For deep neutral PBL, the "launching height" of waves is more likely to be the top of the PBL than the topography itself. A theory is currently sketched by A. Broad (UKMO) to account for this effect.
- in many occasions, low-level blocking is partly resolved by the host model. There is then a double-counting problem for this part of the drag
- The behavior of the schemes in the stratosphere is not sufficiently well understood.

8. Overview of the mesoscale alpine programme

The Mesoscale Alpine Programme (MAP) is a measured response of the international atmospheric and hydrologic community to the challenge of improving the understanding and prediction of intense weather in mountainous areas. It was the first Research and Development Project of the newly created World Weather Research Program of the World Meteorological Organization.

The MAP Special Observing Period (MAP-SOP) took place from 7 September to 15 November 1999. The SOP was funded by many European and North-American weather services and science agencies. The SOP was organized into eight Scientific Projects, referred to as P1 to P8, which were, to some extent, in competition for access to the main facilities. Given here is a brief outline of these projects. A complete list of detailed scientific questions can be found in the MAP Science Plan (Bougeault et al., 1998).

* Project P1 (Orographic Precipitation Mechanisms), addressed the basic mechanisms of production or enhancement of precipitation by topography. It involved studies of the small scale dynamics of precipitating systems, including convective systems and their interaction with the topography, and studies of the detailed growth mechanisms of precipitation particles.

* Project P2 (Incident Upper-Tropospheric PV Anomalies), focused on the dynamics of the large potential vorticity anomalies approaching the Alps from the West at the tropopause level, also called PV-streamers. The role of these anomalies as precursors of severe precipitation in the Alps was investigated, along with their modification by the diabatic heating due to the Alpine precipitation and the significance of small-scale structures seen on water-vapor satellite images.

* Project P3 (Hydrological Measurements and Flood Forecasting), explored the near-real time forecasting capabilities of hydrological flood models, forced by special precipitation measurements or by mesoscale meteorological models. The testing of soil moisture monitoring techniques, the significance of soil moisture initial conditions, and the impact of information on water storage in power company reservoirs were particularly examined.

* Project P4 (Dynamics of Gap Flow), investigated the three-dimensional velocity distribution at the Brenner Pass and within the Wipp Valley, and its time and space variability in relation to the flow above mountain top. The data address some key questions of stratified fluid dynamics, such as the possible formation of a hydraulic jump downstream of the gap, and the consequences of this jump.

* Project P5 (Non-stationary Aspects of Foehn in a Large Valley), addressed the four-dimensional variability of the Foehn flow in the Rhine Valley. It investigated several dynamical processes which determine the spatial extension and time variations of the Foehn, such as the modification of the air mass by radiation, and the interaction with the upper-level flow.

* Project P6 (Three-Dimensional Gravity Wave Breaking), sought answers to the basic questions regarding the creation of clear-air-turbulence by breaking gravity waves, such as the space and time distribution of GWB, the predictability of gravity waves by mesoscale models, the vertical distribution of momentum fluxes in the presence of breaking gravity waves, and the associated potential vorticity generation. It also used new experimental observational strategies, combining remote-sensing and in situ techniques.

* Project P7 (Potential Vorticity Banners),investigated the high resolution structure of the Alpine wake at or below mountain-top level. Numerical models suggest that the wake is organized in well defined potential vorticity banners, extending downstream over several hundred kilometers. The existence and the cross-stream spatial scale of these flow structures were documented.

* Project P8 (Structure of the Planetary Boundary Layer over Steep Orography), sought answers to a number of broad questions on the structure of the orographic PBL, such as its depth and evolution, the three-dimensional distribution of turbulent fluxes within a steep valley, the interaction of PBL turbulence with the local winds, and the exchange of air mass and atmospheric constituents between the PBL and the free troposphere.

In terms of ground systems, MAP was probably the largest field experiment ever conducted in Europe. The field activities were concentrated in three target areas. The Lago Maggiore Target Area (LMTA) was the main focus of projects P1 and P3 (so-called Wet-MAP), as well as part of P8. The Brenner Target Area was the focus for Project P4, and the Rhine Valley Target Area was the focus for Project P5 and part of P8. The remaining projects (P2, P6, and P7) were not linked to specific geographical areas, as they relied mainly on aircraft measurements.

Forecasts for MAP operations were provided by an international team of 25 forecasters working in shifts at the MAP Main Operation Centre (MOC) in Innsbruck. They relied on a variety of model products, satellite and radar pictures, to issue daily forecasts tailored to the needs of mission planning. Forecasting support was also available at the Project Operation Centre (POC) in Milano, especially for nowcasting.

The national and regional meteorological services of the Alpine countries made an outstanding effort to respond to the data and forecast needs of MAP. This is illustrated by the network of operational and research radars and by the network of upper air measurements by radiosondes and wind profilers. Also impressive was the real time exchange of surface data from automated stations, which outnumbered normal GTS requirements by a factor of ten or more. All these data are already available from the MAP Data Center without any restriction.

Several special products were also available to MAP forecasters and scientists during the SOP. Rapid scans (5 minutes) of the METEOSAT-6 stand-by satellite over the Alpine region were activated by EUMETSAT for 24-hour periods, on request from the MAP Operation Center. These covered most of the Intensive Observation Periods (IOPs). A special "Alpine Radar Composite" was produced by DLR with data from all operational radars around the Alps. It was made available through the Internet within 30 minutes from observations. By special agreement of most operational atmospheric electricity networks, enhanced data on lightning were transmitted in real time to ALDIS (Vienna). These were used to compute more precise locations of lightning strikes all over the Alps by combining information from the national networks. This information was displayed on the operational Austrian system in the MOC and was accessible to MAP forecasters.

Finally, a special Numerical Weather Prediction suite was run to provide very high resolution forecasts at the Alpine scale. The meso-scale Canadian AES MC2 model was run at the horizontal resolution of 3km and forced by initial and boundary conditions from the operational model of MeteoSwiss. The model was run every night at the Swiss Center for Scientific Computing in Manno (Switzerland) for the period 21UTC of the previous day to 2400UTC (i.e., a time window of 27 hours). Detailed forecasts of precipitation, wind, turbulence, and potential vorticity were available on horizontal and vertical cross-sections of interest, and were used by mission scientists to optimize the flight plans of the day. The detailed verification of MC2 forecasts was a central objective of several scientific projects. In addition, various model runs (e.g. BOLAM, COAMPS, MM5, MC2 at lower resolution, etc...) were made available to MAP forecasters and scientists through the Internet.

In summary, 17 IOPs were conducted, totaling 42 days of activity. All available resources (in terms of sondes, flight-hours, etc..) were exhausted by the end of the SOP. The statistical evaluation shows that the

year 1999 was a very good year relative to the frequency and distribution of MAP-relevant weather events. All phenomena occurred more frequently than expected relative to the average of the last ten years.

Since the end of the SOP, a high pace of activity has been sustained. Four data managers are currently working at the MAP Data Center to incorporate data received from various research groups in the MAP data base, accessible to anyone through the Internet. The main MAP committees met in Slovenia in May 2000 in the framework of the annual MAP meeting, in Austria in September 2000, and in Germany in May 2001. Early results of the SOP have been presented at several conferences (EGS annual assembly, MAP meetings, AMS/Mountain Meteorology Conference, and International Conference on Alpine Meteorology). A summary paper of the SOP (Bougeault et al., 2001) has appeared in the Bulletin of the American Meteorological Society in March 2001.

For more details and an access to data and literature, see the MAP Internet Site at http://www.map.ethz.ch

9. Possible use of map for SSO parameterizations

The most promising projects from the point of view of SSO parameterizations are P4, P5, P6 and P7. Under P4, detailed measurements where taken within the Wipp valley, a narrow valley joining the Brenner pass to the main valley of the Inn. Micro-barograph measurements are available along this axis, along with 3D velocity measurements by Lidars and aircraft. Figure 7 shows an example where data from the nadir-looking LEANDRE Lidar, on-board the French Fokker 27 aircraft, allow to suspect a transition from sub-critical flow to super-critical flow.

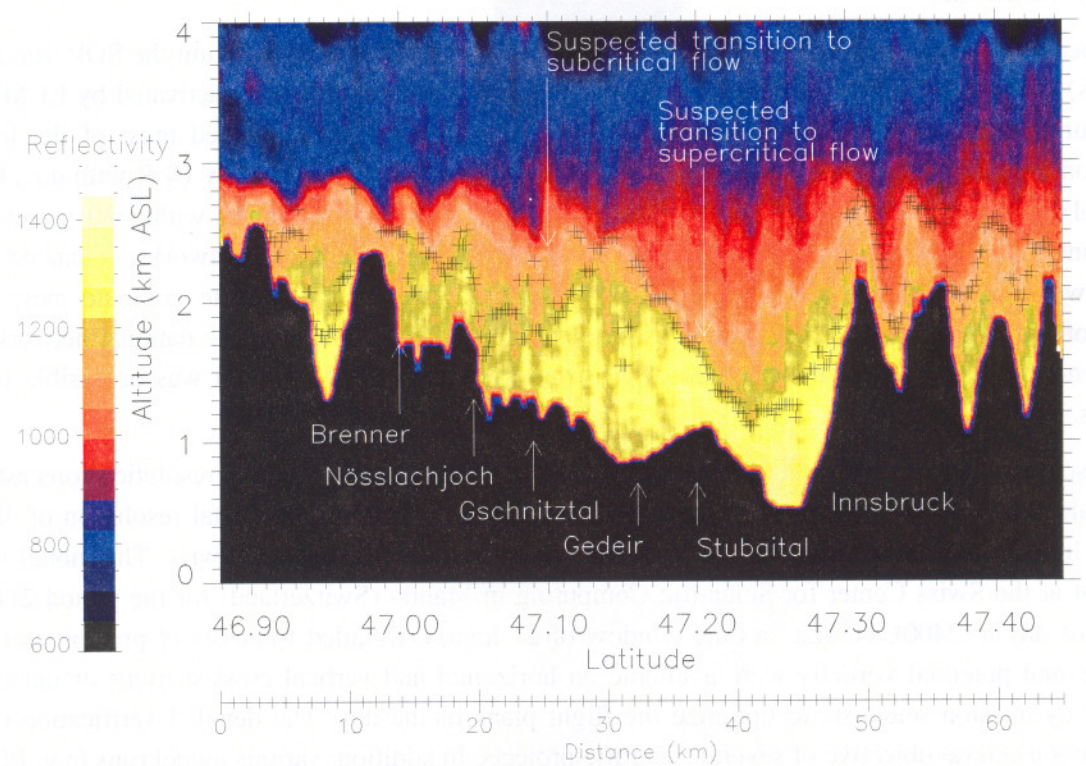

Figure 7: LEANDRE Lidar vertical cross-section of the PBL flow in the Wipp valley on 30 October 1999. The yellow colors trace an aerosol mixed layer. The flow is from left (south) to right (north). Courtesy of C. Flamant.

In P5, many flights of the Merlin aircraft above the Rhine valley allowed to explore the structure and intensity of the turbulence above the Foehn layer, while numerous radio-soundings along the valley are available. Scanning lidars where also operating in the Rhine valley. In P6, a number of flights of several research airplanes provided lee waves measurements. A coordinated flight above the Mont-Blanc gave access to a detailed picture of the 3D, V-shaped wave pattern developing above a layer of stagnant flow in the valley. In P7, flights in the wake of the Alps verified the existence and intensity of jets downstream of the main gaps.

Acknowledgements: A. Brown, S. Webster, M. Miller, B. Ritter, K.I. Kuma, B.A. Boville, T. Hogan and J.F. Geleyn provided useful information about current versions of parameterizations used in their respective centers.

References

Baines, P., 1995: *Topographic effects in stratified flows*. Cambridge University Press, 482pp.

Baines, P. and T.N. Palmer, 1990: Rationale for a new physically_based parameterization of sub-grid scale orographic effects. *ECMWF, Research Department Technical Memorandum No.169.*

Beau, I., 1997: La prise en compte du relief sous-maille dans les modèles météorologiques. *Note 59 of CNRM/GMME*, 95pp (in french).

Beau, I., and P. Bougeault, 1998: Assessment of gravity wave drag parameterizations with PYREX data. *Quart. J. Roy. Meteor. Soc.*, **124**, 1443-1464.

Bessemoulin, P., P. Bougeault, A. genoves, A. Jansa Clar, and D. Puech, 1993 : Mountain pressure drag during PYREX. *Contrib. Atmos. Phys.*, **66**, 305-325.

Boer, G.J., N.A. McFarlane, and R. Laprise, 1984: The Canadian Climate center spectral atmospheric general circulation model. *Atmosphere-Ocean*, **22**, 397-429.

Bougeault, P., I. Beau, and J. Stein 1993: Validation of Meteorological models and parameterizations with observations of the PYREX experiment. ECMWF Seminar *Proceedings, Validation of models over Europe, 7-11 September 1992*, Volume 1, 247-285.

Bougeault, P., et al., 1997 : PYREX : A summary of findings. *Bull. Amer. Meteor. Soc.*, **78**, 637-650.

Bougeault, P., P. Binder and J. Kuettner, 1998: *MAP Science Plan*. Available from http://www.map.ethz.ch

Bougeault, P., P. Binder, A. Buzzi, R. Dirks, R. Houze, J. Kuettner, R.B. Smith, R. Steinacker and H. Volkert, 2001: The MAP Special Observing Period. *Bull. Amer. Meteor. Soc.*, **82**, 433-461.

Emeis, S., 1990: Surface pressure distribution and pressure drag on mountains. *International Conference on Mountain Meteorology and ALPEX, Garmish-Partenkirchen*, 5-9 June, 1989, 20-22.

Georgelin, M., E. Richard, M. Petitdidier, and A. Druilhet, 1994: Impact of sub-grid scale orography parameterization on the simulation of orographic flows. *Mon. Wea. Rev.*, **122**, 1509-1522.

Georgelin, M., et al., 2000: The second COMPARE exercise: a model inter-comparison using a case of a typical meso-scale orographic flow, the PYREX IOP3. *Quart. J. Roy. Meteor. Soc.*, **126**, 991-1029.

Gill, A, 1982: *Atmosphere-Ocean Dynamics*. Academic Press.

Grant, A.L.M., and P.J. Mason, 1990: Observations of boundary layer structure over complex terrain. *Quart. J. Roy. Meteor. Soc.*, **116**, 159-186.

Gregory, D., G.J. Shutts and J.R. Mitchell, 1998: A new gravity-wave drag scheme incorporating anisotropic orography and low-level wave breaking: Impact upon the climate of the UK Meteorological Office Unified Model. *Quart. J. Roy. Meteor. Soc.*, **124**, 463-493.

Héreil, P., and J. Stein, 1997: Momentum budgets over idealized orography with a non-hydrostatic anelastic model. *ECMWF Workshop on Orography*, pp 117-136.

Héreil, P. and J. Stein, 1999: Momentum budgets over idealized orography with a non-hydrostatic anelastic model. I: two-dimensional flows. *Quart. J. Roy. Meteor. Soc.*, **125**, 2019-2051.

Héreil, P. and J. Stein, 1999: Momentum budgets over idealized orography with a non-hydrostatic anelastic model. II: two-dimensional flows. *Quart. J. Roy. Meteor. Soc.*, **125**, 2053-2073.

Kustas, W.P., and W. Brutsaert, 1986: Wind profile constants in a neutral atmospheric boundary layer over complex terrain. *Bound.-Layer Meteor.*, **34**, 35-54.

Lindzen, R.S., 1981: Turbulence and stress owing to gravity wave and tidal breakdown. *J. Geophys. Res.*, **86**, 9707-9714.

Lott, F., 1999: Alleviation of stationary biases in a GCM through a mountain drag parameterization scheme and a simple representation of lift forces. *Mon. Wea. Rev.*, **127**, 788-801.

Lott, F. and M. Miller, 1997: A new sub-grid scale orographic drag parameterization: Its formulation and testing. *Quart. J. Roy. Meteor. Soc.*, **123**, 101-127.

Mason, P.J., 1986: On the parametrization of orographic drag. *ECMWF Seminar on Physical Parametrizations for Numerical Models of the Atmosphere*, pp. 139-165.

McFarlane, N.A., 1987: The effects of orographically excited gravity waves on the general circulation of the lower stratosphere and troposphere. *J. Atmos. Sci.*, **44**, 1775-1800.

Mesinger, F., 1977: Forward-backward scheme and its use in a limited-area model. *Contrib. Atmos. Phys.*, **50**, 200-210.

Mesinger, F., and W. Collins, 1986: Review of the representation of mountains in numerical weather prediction models. In *ECMWF Seminar/Workshop on Observation, Theory and Modelling of Orographic Effects*, Vol.2, pp.1-28.

Mobbs, S., 1995: The parametrization of sub-grid scale orography. In *ECMWF Seminar on Parametrization of Sub-Grid Scale Processes*, 5-9 September 1994, pp. 305-324.

Olafsson, H., and P. Bougeault, 1997: The effect of rotation and surface friction on orographic drag. *J. Atmos. Sci.*, **54**, 193-210.

Palmer, T., G.J. Shutts and R. Swinbank, 1986: Alleviation of a systematic westerly bias in general circulation and numerical weather prediction models through an orographic gravity wave drag parameterization. *Quart. J. Roy Meteor. Soc.*, **112**, 1001-1039.

Phillips, D.S., 1984: Analytical surface pressure and drag for linear hydrostatic flow on three-dimensional elliptical mountains. *J. Atmos. Sci.*, **41**, 1073-1084.

Queney, P., 1948: The problem of air flow over mountains: A summary of theoretical studies. *Bull. Amer. Meteor. Soc.*, **29**, 16-26.

Satomura, T., 1996: Supplement to "Numerical simulation of lee-wave events over the Pyrénées". *J. Meteor. Soc. Japan*, **74**, 147-153.

Shutts, G.J. and A. Gadian, 1997: Critical level filtering of orographic gravity waves in directional wind shear. *ECMWF Workshop on Orography*, pp 97-115.

Smith, R.B., 1979: Some aspects of quasi-geostrophic flow over mountains. *J. Atmos. Sci.*, **36**, 2385-2393.

Taylor, P.K., et al., 1997: Boundary-layer modelling of neutral and stably stratified flow over hills, with emphasis on the drag. *ECMWF Workshop on Orography*, pp. 1-21.

Wallace, J.M., S. Tibaldi and A.J. Simmons, 1983 : Reduction of systematic errors in the ECMWF model through the introduction of an envelope orography. *Quart. J. Roy Meteor; Soc.*, **109**, 683-717.

Wood, N., and P.J. Mason, 1993: The pressure force induced by neutral, turbulent flow over hills. *Quart. J. Roy. Meteor. Soc.*, **119**, 1233-1267.

Workshop on Orography, Proceedings, ECMWF, 10-12 November 1997, available from ECMWF.